Overview of Aquarius Radiometer Post-Launch Measurements Counts to Antenna Temperature Processing for Product Version 5

Paolo de Matthaeis
Jinzheng Peng
Jeffrey Piepmeier
David Le Vine

1. Introduction

This document provides an overview of the algorithms used to transform raw Aquarius radiometer acquisitions into antenna temperature data. The main steps followed in this processing are:

1. non-linearity correction,
2. antenna gain glitch detection,
3. computation of internal gains and offsets,
4. radio-frequency interference (RFI) algorithm and coefficients,
5. transformation into antenna temperature,
6. front-end loss correction.

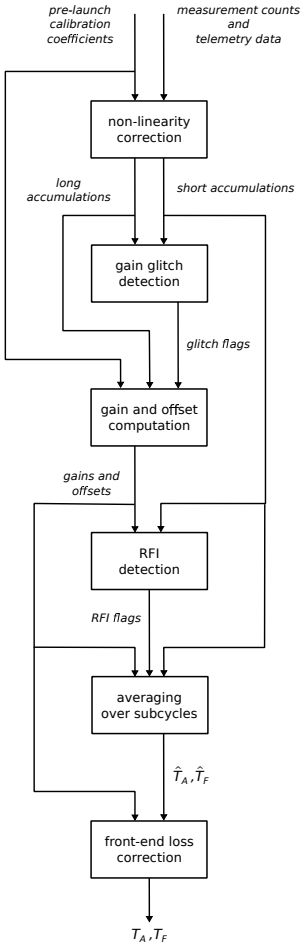

Figure 1.1: *Counts to T_A flow diagram.*

An operational flow diagram showing these stages is given in Figure 1.1.

The Aquarius radiometer measures the first three Stokes parameters by sensing four polarizations: vertical (v), horizontal (h), linear $+45^o$ (p), and linear -45^o (m). The raw measurements (L1-level data) undergo an initial correction for non-linearity in the receiver (see Section 3). The data corrected for non-linearity enter a glitch detector, as explained in Section 4, and then are fed to the RFI detection algorithm (Section 6) which also requires calibrated gain and offset (Section 5). The RFI flags are then used when generating the output data averaged over 1.44 s, both with samples identified as RFI removed ($\hat{T}_F$) and samples with

no RFI mitigation ($\hat{T}_A$)(Section 7). Finally, these products are corrected for front end losses and phase imbalance to yield the mitigated and un-mitigated antenna temperatures, T_F and T_A respectively (Section 8).

The receiver comprises a reflector, three feed horns, ortho-mode transducers (OMT), correlated noise diode (CND) networks, diplexers, and radio-frequency (RF) front- and back-ends (RFE and RBE). The radiometric loss model for the receiver is shown in Figure 1.2 (from [1]).

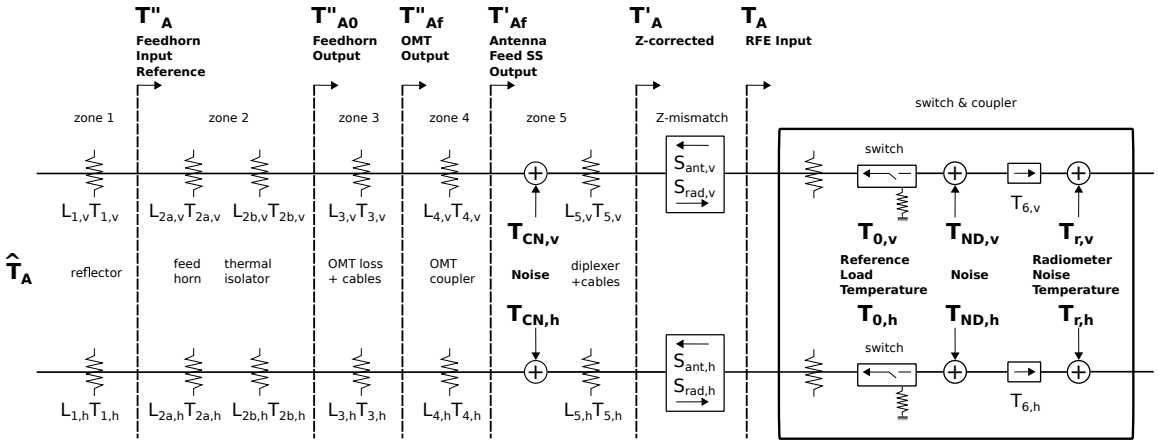

Figure 1.2: *Loss model used for the Aquarius radiometer receiver.*

Front-end loss and impedance mismatch corrections must be applied to propagate the internally calibrated noise temperature T_A (at the RFE input plane) forward to the apparent aperture temperature $\hat{T}_A$ (at the reflector input). The antenna and electronics subsystems are separated by the so-called OMT coupler, which is used for injecting CND noise power into the RF path. The RFE contains Dicke (or reference load) switches and noise diodes coupled independently into each of the v- and h-polarization channels. The v- and h-polarization signals are combined in a 180^o hybrid coupler to generate p- and m-polarization signals. These four signals are detected by tunnel diodes and integrated in 10 ms units. The RFE cycles through a combination of antenna, reference load, and noise diode looks to produce the data necessary for internal opertional calibration of the electronics.

2. Acquisition Scheme and Data Structure

The three radiometers, one for each antenna, operate in parallel. Each of them performs a measurement every 10 ms. In nominal operation, during 120 ms (one subcycle) each radiometer collects seven samples every 10 ms looking into the antenna followed by five samples devoted to the calibration sources. The calibration sources are two noise diodes (ND) and a Dicke load (DL) [1]. One cycle of a radiometer measurement contains 12 subcycles [2]. Figure 2.1 shows how the samples corresponding to one antenna temperature value are organized. Within each 120 ms subcycle, the first and second and the third and fourth 10 ms acquisitions are added together to produce two equivalent 20 ms samples. As a

results, each subcycle contains five antenna measurements, also called short accumulations (SA), recorded at the start of the cycle and 20 ms, 40 ms, 50 ms, and 60 ms afterwards, and five calibration (non-antenna) measurements.

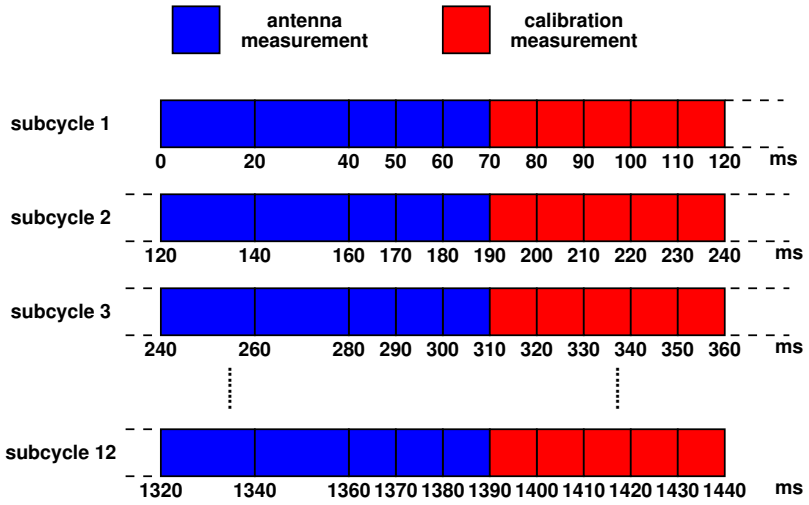

Figure 2.1: *Structure of a measurement cycle.*

The measurements acquired looking at the noise diodes and Dicke load in eight different configurations are averaged over longer periods (1.44 s) for the use of internal calibration and are called long accumulations (LA). RFI detection and mitigation needs long accumulations in order to determine calibration gains and offsets.

3. Non-Linearity Correction

Radiometer counts are corrected in order to remove receiver non-linearity over the bright range of measured brightness temperature. Correction coefficients and their temperature dependencies were measured during pre-launch calibration testing at Goddard Space Flight Center (GSFC). The correction algorithm operates directly on the uncalibrated detector count values from the radiometer. These detector count values V are synonymous with the short accumulations (SA1 to SA6) and long accumulations (LA1 to LA8) values normalized to a single-step accumulation. The linearized count value v_d is expanded into a polynomial of raw counts V:

$$v_d = V + c_2 V^2 + c_3 V^3 \tag{3.1}$$

The expansion coefficients c_2 and c_3 are written as functions of physical temperature:

$$c_2 = c_{2,0} + c_{2,1}\,\Delta T + c_{2,2}\,\Delta T^2 \tag{3.2}$$

$$c_3 = c_{3,0} + c_{3,1}\,\Delta T + c_{3,2}\,\Delta T^2 \tag{3.3}$$

where

$$\Delta T = T_D - T_{ref} \tag{3.4}$$

is the deviation of the detector temperature T_D from the reference temperature T_{ref}. The reference temperature was determined by polynomial model fitting of test data, with one set of coefficients needed for each radiometer channel, as described in the Pre-Launch Calibration Test Report [3].

4. Aquarius Radiometer Gain Jitter Detection Algorithm

The Aquarius radiometers represented the state of the art in stability and internal calibration, and this was one of the reasons Aquarius was successful at measuring sea surface salinity and meeting its scientific goals. However, at the time of the development and testing of the Aquarius radiometers, it was noticed that occasionally during smooth changes in temperature, the gain varied suddenly rather than gradually as if the radiometer had moved to a different state. These sudden variations were called gain "glitches" or gain "jitter". Once in equilibrium, the radiometer was very stable, but as a precaution, a filter was developed to identify and flag these anomalies. This is the box labelled "Gain Glitch Detection" in the system block diagram of Figure 1.1. When a gain glitch is flagged by the detector, a smoothing window for both gain and offset is used to replace the abrupt transition.

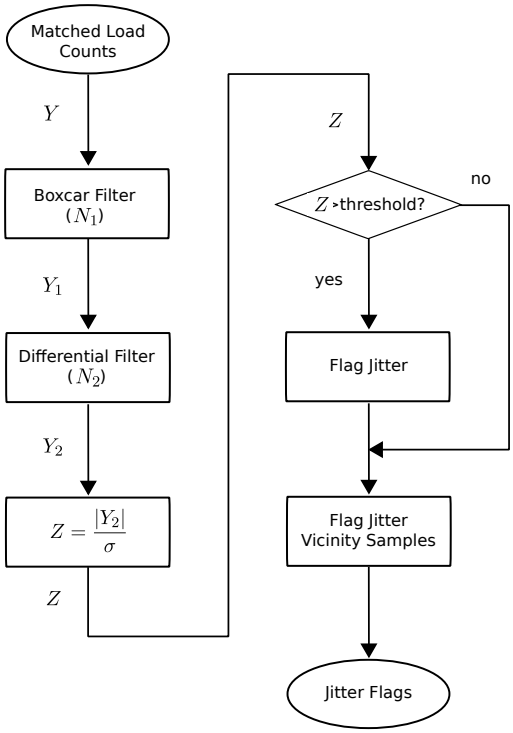

Figure 4.1: *Gain jitter detection algorithm.*

The gain jitter is detected according to the flow chart in Figure 4.1. The input data used for the algorithm are the matched load counts. Details are given in Appendix A. Glitches occurred very rarely in the nearly four years of Aquarius operation.

5. Computation of Internal Gains And Offsets

Aquarius uses a noise diode for internal calibration. The gain and offset coefficients for the linear polarization channels V and H are computed using the Dicke load and noise diode through the expressions

$$g = \frac{v_d(DL+ND) - v_d(DL)}{T_{ND}} \tag{5.1}$$

$$o = v_d(DL) - g\,T_0 \tag{5.2}$$

where T_{ND} is the excess noise temperature of the noise diode, T_0 is the Dicke load temperature and the linearized count values (see Section 3) for the measurements of the Dicke load $v_d(DL)$ and Dicke load + noise diode $v_d(DL+ND)$ are

$$v_d(DL) = \begin{cases} \frac{1}{2}\left[v_d(LA1/10) + v_d(LA4/10)\right] & \text{for V-polarization} \\ \frac{1}{2}\left[v_d(LA1/10) + v_d(LA2/10)\right] & \text{for H-polarization} \end{cases} \tag{5.3}$$

$$v_d(DL+ND) = \begin{cases} \frac{1}{2}\left[v_d(LA2/10) + v_d(LA3/10)\right] & \text{for V-polarization} \\ \frac{1}{2}\left[v_d(LA3/10) + v_d(LA4/10)\right] & \text{for H-polarization} \end{cases} \tag{5.4}$$

More details are given in section 4 of [1]. The calculation of the gain and offset coefficient for the p- and m-polarization channels is more complicated and can be found in section 5 of [1].

6. RFI Detection

The raw antenna measurements in Figure 6.2 are processed to reduce the effect of Radio Frequency Interference (RFI) before being converted to antenna temperatures. The Aquarius RFI algorithm assumes a signal with a normal distribution in the RFI-free environment and detects RFI by identifiying individual samples of the antenna temperature (short accumulations) that deviate significantly from the average value of nearby samples. Mitigation is accomplished in subsequent processing steps by excluding corrupted samples before averaging them to yield the antenna temperatures (see Section 7). Some stages also require calibration gains and offsets, that are computed based on the long accumulations. Individual samples of the correlated noise diode counts are also flagged as corrupted RFI if they are near an antenna temperature sample that has been flagged. The algorithm is performed independently for each radiometer channel. All input and output data and dynamic auxiliary data are processed independently for each polarization. Accordingly, independent versions of all static auxiliary data files are maintained for each polarization and each radiometer.

Before being fed to the RFI Detection Algorithm, the string of data shown in Figure 2.1 undergoes some pre-processing. After the correction for non-linearity of the receiver, the first two short accumulations, which represent 20 ms of data, are divided by 2 and counted twice. In addition, zeros are applied when no antenna measurements were taken, such as during the intervals of internal calibration. Therefore, for each subcycle of 120 ms, the

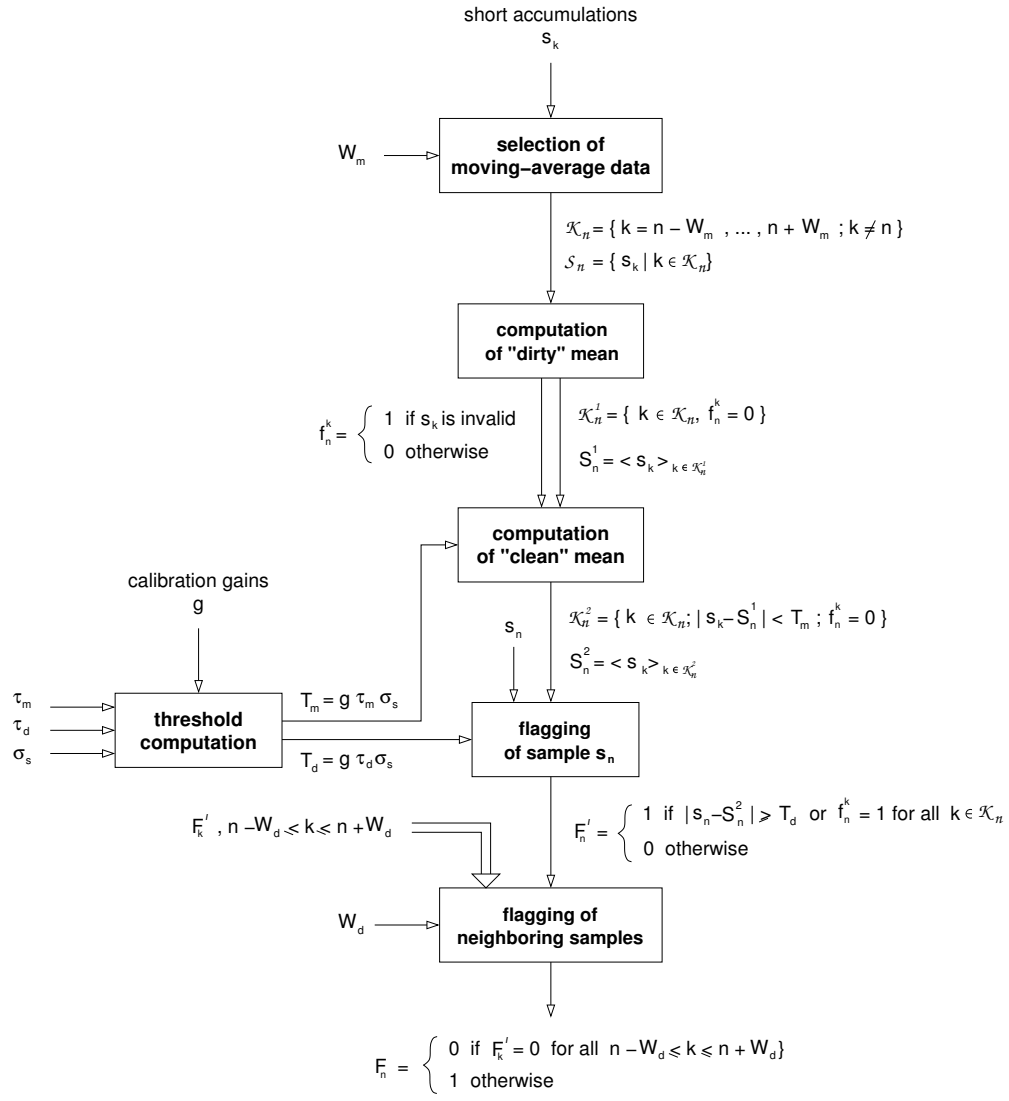

Figure 6.1: *Flow diagram for Aquarius radiometer RFI detection algorithm.*

result is a string of seven 10-ms spaced values $s_n (n = 1, 2, \ldots, 7)$ representing the short accumulations, followed by five zeros, $s_n (n = 8, 9, \ldots, 12)$, representing the intervals devoted to calibration, as shown in Figure 6.2 (left). A correction for the non-linearity of the receiver is also applied to these samples $s_n (n = 1, 2, \ldots, 7)$. Since there are twelve subcycles in each 1.44 s block, a total of $7 \times 12 = 84$ non-zero 10 ms antenna samples are taken for each data point. All the strings are lined up in temporal order to form a continuous stream of values that are then used by the RFI detection algorithm.

After launch, it was noticed that the first short accumulation (20 ms sample) had values inconsistent with the other short accumulations. Therefore, as a precaution, it has been excluded from the subsequent data processing. As a results, the data that are used for RFI detection and mitigation are as shown in Figure 6.2 (right), with the two equivalent 10 ms samples corresponding to the first short accumulation of each subcycle being replaced

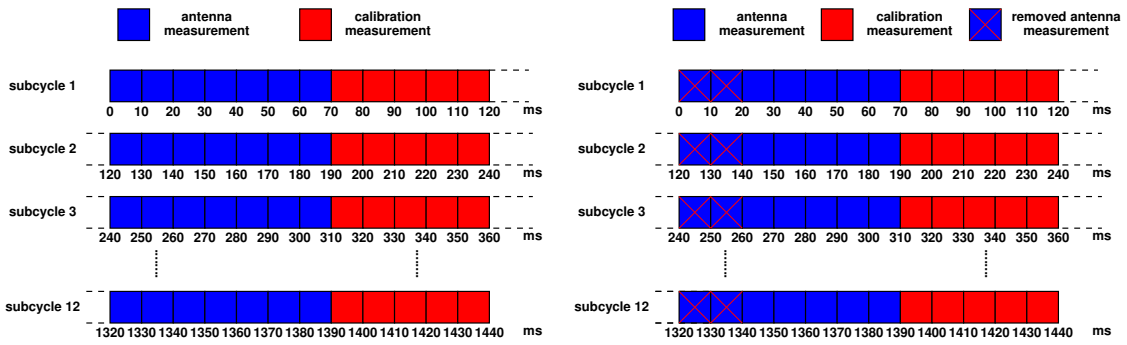

Figure 6.2: *Equivalent data string with 10 ms samples, with all measurements (left) and samples corresponding to the 20 ms first short accumulation removed (right).*

by zeros. Only the samples $s_n(n = 3, 4, 5, 6, 7)$ are used for each subcycle, for a total of $5 \times 12 = 60$ non-zero 10 ms antenna samples per 1.44 s cycle.

The steps in the RFI detection algorithm are shown in the flow chart of Figure 6.1. The test for presence of RFI is applied to each valid sample (i.e. each value that corresponds to an antenna measurement) in the data stream. The algorithm consists of the following steps.

1. **Selection of samples to be averaged together to estimate local mean:** A set consisting of W_m samples surrounding the sample under test is extracted from the data stream and used to estimate the local mean value of the short accumulations.

2. **Computation of "dirty" mean:** A "dirty" mean is computed using all samples in this data set.

3. **Computation of "clean" mean:** A "clean" (in the sense of being free of outliers) mean is calculated using only those samples that deviate from the dirty mean by less than a threshold T_m.

4. **Testing samples for presence of RFI:** Each sample is compared to the corresponding clean mean and if it differs from it by more than a threshold T_d in absolute value, then it is considered to be RFI.

5. **Flagging samples on the neighborhood of RFI-flagged samples:** Samples within $\mp W_d$ steps on either side of the sample under test are considered tainted and also flagged as RFI.

Five independent static parameters are used, i.e., τ_m, τ_d, W_m and W_d, σ_s. The threshohlds T_m and T_d can be found from σ_s, tau_m, τ_d and the gain g using the expressions

$$T_m = \tau_m \, \sigma_s \, g \tag{6.1}$$

$$T_d = \tau_d \, \sigma_s \, g \tag{6.2}$$

The values of the first four parameters are

$$\tau_m = 1.5, \; \tau_d = 4.0, \; W_m = 20, \; W_d = 2 \tag{6.3}$$

The parameter σ_s varies with polarization and radiometer beam, and its values are chosen to be close the standard deviation of the antenna temperatures measured over RFI-free ocean. It can assume two different values, which are listed in Table 6.1. More details on the Aquarius radiometer RFI detection algorithm can be found in [4],[5].

	σ_s over ocean				σ_s over land and sea ice			
beam	V	+90°	−90°	H	V	+90°	−90°	H
1 (inner)	0.558	0.551	0.540	0.532	0.720	0.731	0.725	0.695
2 (middle)	0.543	0.562	0.548	0.538	0.707	0.726	0.737	0.709
3 (outer	0.552	0.548	0.554	0.546	0.720	0.763	0.740	0.717

Table 6.1: *Values of parameter σ_s (V = vertical polarization, H = horizontal polarization).*

7. RFI Mitigation and Conversion to Antenna Temperatures

RFI mitigation is accomplished by removing, in the conversion to antenna temperature values, all short accumulations flagged as corrupted by RFI. All presumed RFI-free short accumulations within a 1.44 s cycle are averaged together and converted to antenna temperatures using the gain and offset. For the linear polarizations V and H, the espressions are

$$\hat{T}_F = \frac{1}{g}\left[\left(\frac{1}{N_F}\sum_{n|F_n=0} s_n\right) - o\right] \tag{7.1}$$

where N_F is the number of short accumulation non flagged as corrupted by RFI in the measurement cycle under consideration. The unfiltered antenna temperature is also computed for reference,

$$\hat{T}_A = \frac{1}{g}\left[\left(\frac{1}{N}\sum_{n} s_n\right) - o\right] \tag{7.2}$$

where N is the total number of short accumulation in the measurement cycle under consideration. The calibration gains g and offsets o are computed using the long accumulations and have different values depending on the particular radiometer and polarization, as mentioned in 5. The expressions for the Third Stokes parameter are more complicated and can be found in section 5 of [1].

8. Front-end Loss Correction

Front-end losses and phase imbalance within the radiometer electronics (see Figure 1.2) reduce the antenna temperature T_A to a $\hat{T}_A$ value. In this step, the radiometer output T_A is obtained from $\hat{T}_A$ as

$$T_{A,p} = L_1\, T''_{A,p} - (L_1 - 1)\, T_1 \qquad \text{for } p = v, h \tag{8.1}$$

$$T_{A,3} = \frac{L_f}{\cos\Delta\phi_f}\,\hat{T}_{A,3} \tag{8.2}$$

where

$$T''_{A,p} = L_{2A,p}\, L_{2B,p}\, T''_{A0,p} - L_{2A,p}\,(L_{2B,p} - 1)\, T_{2B} - (L_{2A,p} - 1)\, T_{2A} \tag{8.3}$$

$$T''_{A0,p} = L_{3,p}\, T''_{Af,p} - (L_{3,p} - 1)\, T_{3,p} \tag{8.4}$$

$$T''_{Af,p} = L_{4,p}\, T'_{Af,p} - (L_{4,p} - 1)\, T_{4,p} \tag{8.5}$$

$$T'_{Af,p} = L_{5,p}\, T'_{A,p} - (L_{5,p} - 1)\, T_{5,p} \tag{8.6}$$

$$T'_{A,p} = L_{MM,p}\, \hat{T}_A - (L_{MM,p} - 1)\, T_{ND,P} \tag{8.7}$$

$$L_f = L_1 \sqrt{L_{2A,v}\, L_{2A,h}} \sqrt{L_{2B,v}\, L_{2B,h}} \left[\prod_{n=3}^{5} \sqrt{L_{n,v}\, L_{n,h}} \right] \sqrt{L_{MM,v}\, L_{MM,h}} \tag{8.8}$$

the OMT / cable sub-assembly pahse imbalance $\Delta\phi_f$ and the loss factors L_1, L_{2A}, L_{2B}, L_3, L_4, L_5 and L_{MM} are defined in [1].

Appendix A Description of Gain Jitter Detection Algorithm

A.1 Introduction

The Aquarius radiometers are polarimetric microwave radiometers. Each of them consists of v, p, m and h polarimetric channels. Three radiometers operate in a pushbroom mode for global sea surface salinity mapping. Due to imperfect components, unexpected gain jitter happens in some polarimetric channels under certain ambient temperatures. To detect the gain jitter automatically during the Aquarius mission, a gain jitter detection algorithm was developed and implemented.

A.2 Algorithm description

The flow diagram of the gain detection algorithm is shown in Figure A.1.

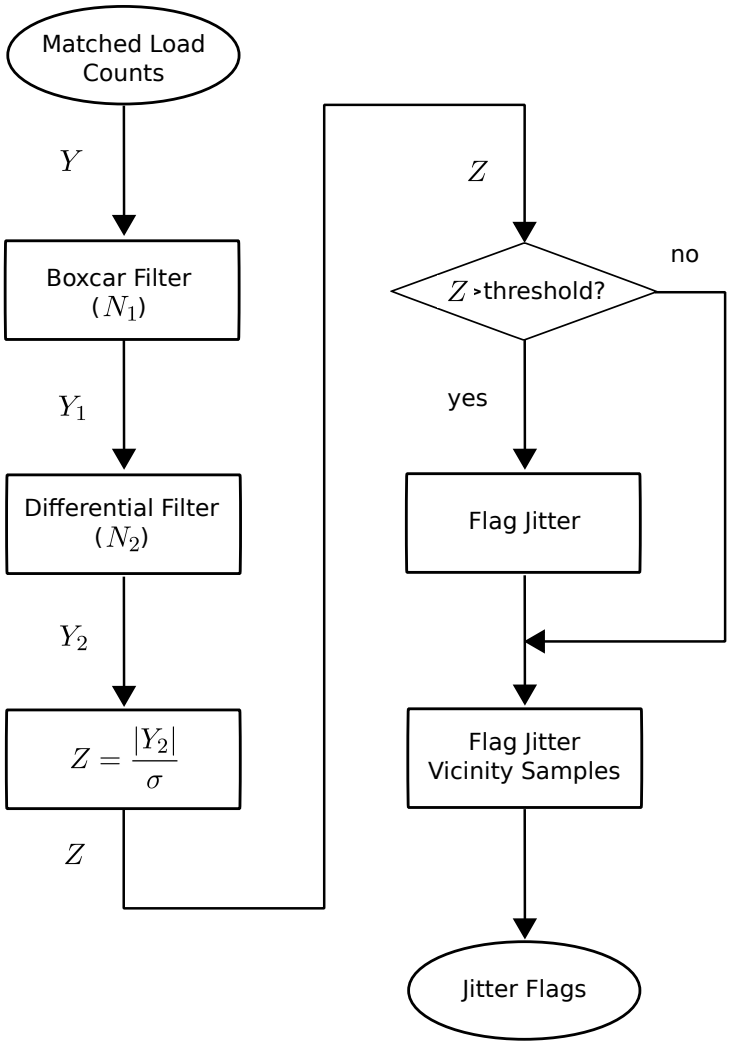

Figure A.1: *Gain jitter detection algorithm.*

The matched load counts are used as input for gain jitter detection because of the stability of the reference load compared to the other sources. The dataset of the matched load counts is processed by two digital filters (a boxcar filter and a differential filter as shown in Figure A.1) in sequence and then the normalized output, Z, is compared to the detection threshold to detect possible gain jitter. The expressions of the two digital filters output are:

$$Y_1(n) = \begin{cases} Y(n) & \text{for } N_1 = 0 \\ \dfrac{1}{N_1} \displaystyle\sum_{k=-(N_1-1)/2}^{(N_1-1)/2} Y(n+k) & \text{for } N_1 > 0\,,\ N_1 \text{ odd} \\ \dfrac{1}{N_1} \displaystyle\sum_{k=-N_1/2}^{N_1/2-1} Y(n+k) & \text{for } N_1 > 0\,,\ N_1 \text{ even} \end{cases} \tag{A.1}$$

$$Y_2(n) = \begin{cases} Y_1\left(n + \dfrac{N_2-1}{2}\right) - Y_1\left(n - \dfrac{N_2-1}{2}\right) & \text{for } N_1 \text{ odd} \\ Y_1\left(n + \dfrac{N_2}{2} - 1\right) - Y_1\left(n - \dfrac{N_2}{2}\right) & \text{for } N_1 \text{ even} \end{cases} \tag{A.2}$$

where N_1 is the length of the boxcar filter and N_2 is the interval between the two samples when the differential filter is used. The impulse response of the filters is shown in Figure A.2.

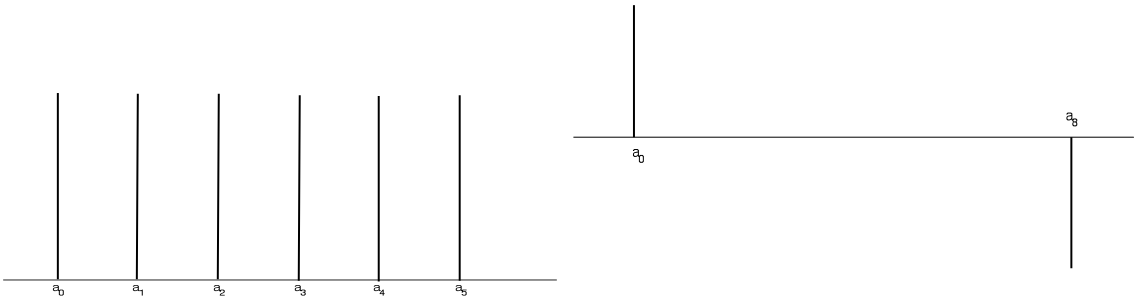

(a) (b)

Figure A.2: *Impulse response of (a) the boxcar filter with $N_1 = 6$ and (b) the differential filter with $N_2 = 8$.*

The absolute value of the output from the differential filter, $|Y_2|$ in Figure reffig:J01, is normalized by its standard deviation σ, i.e.,

$$Z = \frac{|Y_2|}{\sigma} \tag{A.3}$$

This normalized output will be compared to the detection threshold. The samples above threshold will be flagged as gain jitters, and $\lfloor N_2/2 \rfloor$ samples before and after each of these flagged samples are also flagged as gain jitters, where $\lfloor x \rfloor$ is the greatest integer that is less

than or equal to x. Optimal values of the filter parameters (N_1 and N_2) and the detection threshold are derived by using training dataset and the approach to derive them is described in Section A.3.

A.3 Filter parameter optimization

The dataset 'GSFC_Orbital_LASAs' (from 2007-12-18 16:40:49 to 2007-12-19 1:59:57) is used as the training dataset to derive the optimal values for the filter parameters and the range of the detection threshold. This dataset includes the following subsets:

- from 2007-12-18 from 16:40:49.0214 to 16:42:09.6932
- from 2007-12-18 from 19:36:32.8791 to 19:37:49.2385
- from 2007-12-18 from 21:06:47.2946 to 21:07:49.2321
- from 2007-12-18 from 22:39:51.8114 to 22:41:02.8739
- from 2007-12-19 from 00:12:27.0050 to 00:13:36.1456
- from 2007-12-19 from 01:43:27.6918 to 01:44:28.1918

In the training dataset, gain jitters only appear in radiometer 2 channel 4 during the following period and they are shown in Figure A.3. The data in the other channels of the 3 radiometers are gain jitter free.

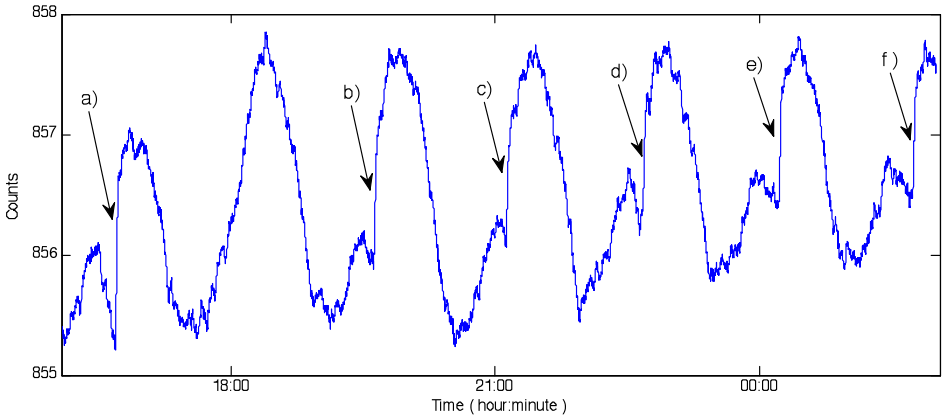

Figure A.3: *Gain jitter location.*

Using the gain jitter free data, the filter parameters (N_1 and N_2) are varied to obtain a reasonable range of the detection threshold. For a given pair of N_1 and N_2, the second largest value of Z in Equation (A.3) is used as the minimum detection threshold (or the lower limit) and the result is shown in Figure A.4(a). The minimum detection threshold and its corresponding filter parameters (N_1 and N_2) are then applied to the gain jitter data to get the gain jitter detection probability and false alarm rate. The results are shown in Figures A.4(b) and A.4(c). Note that the filter parameters in Figure A.4 are the Boxcar filter width W_{BF} and the sample interval T_S obtained as

$$T_s = \frac{t_s(N) - t_s(1)}{N - 1} \tag{A.4}$$

where t_s is the time tag of the samples. They are expressed in seconds and their relation to the parameters N_1 and N_2 is given by:

$$N_1 = \text{round}\left(\frac{W_{BF}}{T_S}\right) \tag{A.5}$$

$$N_2 = \max\left(\frac{W_{BF}}{\Delta T}, 1\right) \tag{A.6}$$

From Figure A.4(b), it can be found that the optimal value of the boxcar filter width is 0 s or $N_1 = 0$ (or $Y_1 = Y$ in Figure A.1, note that the value of the parameter T_S in the dataset is 60 s). $N_1 = 0$ is optimal so that N_2 can be as small as possible because samples before and after a flagged sample will be flagged as gain jitter. The value of N_2 is chosen to be 2 to balance the detection probability in Figure A.4(b) and the false alarm rate in Figure A.4(c).

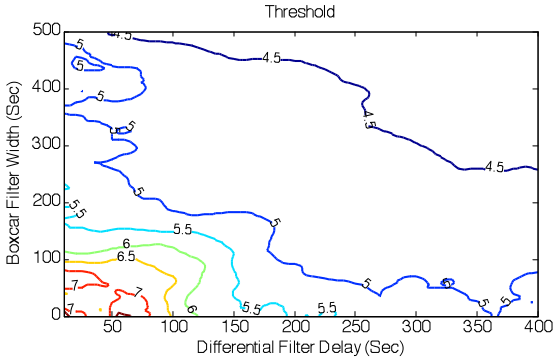

(a): Minimum detection threshold

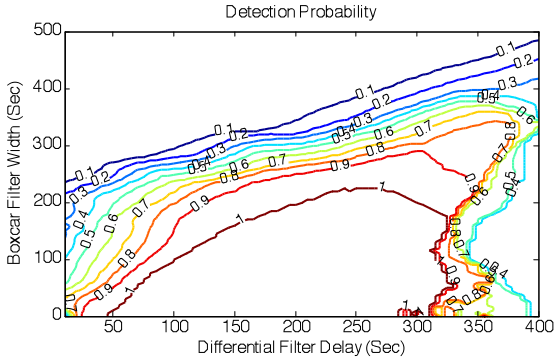

(b): Detection probability with detection threshold from (a)

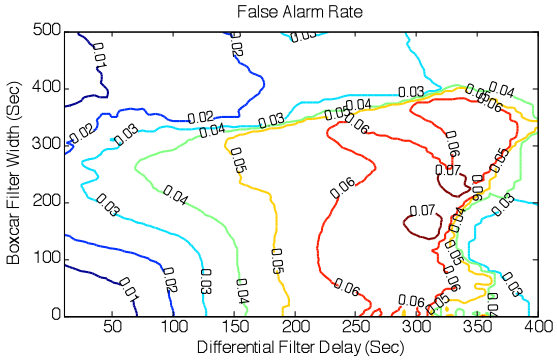

(c): False alarm rate with detection threshold from (a)

Figure A.4: *The relationship among the filter parameters, minimum detection threshold and their corresponding detection performance.*

After the filter parameters (N_1 and N_2) are chosen, the gain jitter data is tested with varied detection threshold to get the upper limit of the detection threshold. The detection

performance (detection probability and false alarm rate) versus detection threshold are shown in Figure A.5. It can be found that the upper limit is 10.3. Therefore, the detection threshold for the gain jitter detection algorithm will vary between 6.5 and 10.3.

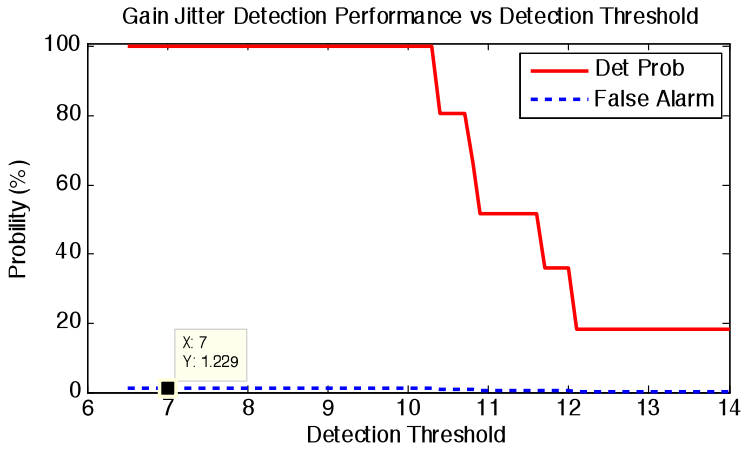

Figure A.5: *Detection probability and false alarm versus detection threshold. X and Y show the coordinates of the square marker on the dash line*

In order to reduce uncertainty in the computation of standard deviation σ in Equation A.3, the size of the dataset under gain jitter detection should be large enough. The relation between the standard deviation and the size of the dataset (in time here) is shown in Figure A.6. The minimum size in time of a dataset under gain jitter detection is recommended to be at least 2 to 3 hours.

A.4 Test result with other data sets

Three additional datasets listed in A.1 are used to test the gain jitter detection algorithm to adjust the range of the detection threshold. Gain jitter free data are used to determine the optimal detection threshold, which is found to be equal to 7. This result is within the range between 6.5 to 10.3 obtained in Section A.3.

Name	Start Time	End Time	Note
JPLradspecial	2009/04/30 20:30:03.1052	2009/05/01 03:29:56.5841	JPL
JPLTV1orbital	2008/10/03 09:00:00.8423	2008/10/03 20:59:59.2353	JPL
GSFCTV2stable	2007/12/17 21:00:30.2092	2007/12/18 11:59:59.7216	GSFC

Table A.1: *Additional test datasets.*

Using the data with gain jitter included, the detection threshold needs to be increased to 8. The test results with detection threshold equal to 8 are listed in Table A.2. The false alarm is less than 0.1%, while all of the gain jitters in gain jitter dataset can be effectively detected and flagged. An example to illustrate the detection is shown in Figure A.7.

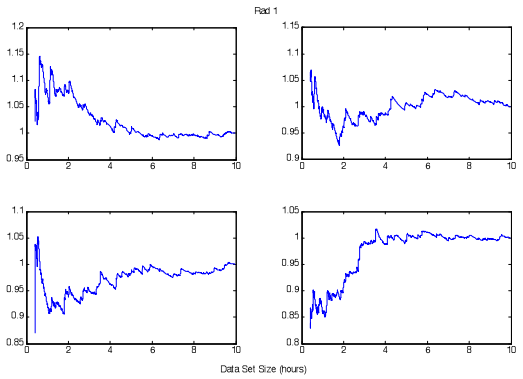

(a): Radiometer 1

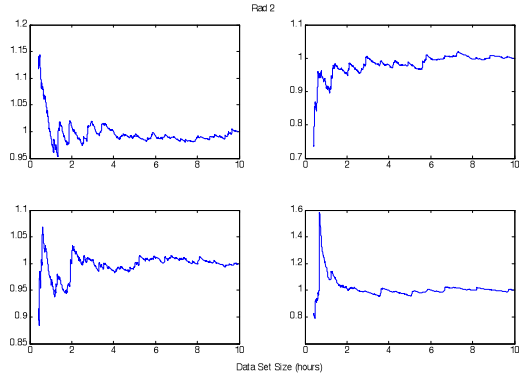

(b): Radiometer 2

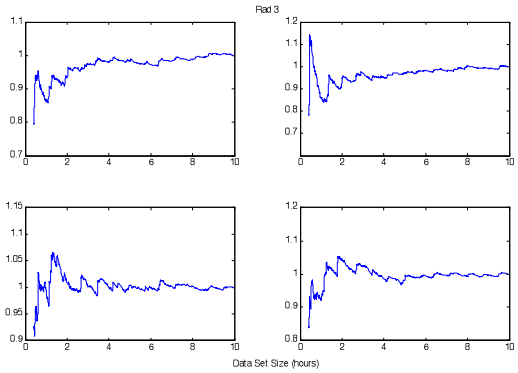

(c): Radiometer 3

Figure A.6: *Normalized standard deviation versus data set size.*

Data Set	Gain Jitter Channel	Non-Gain Jitter Channel	Total Samples	False Alarm	Gain Jitter Detection
JPLradspecial	Rad 1: Ch 1,4 Rad 2: Ch 4		52242		See Figure A.5
		Rad 1: Ch 2,3 Rad 2: Ch 1-3 Rad 3: Ch 1-4	156726	$< 0.1\%$	
JPLTV1orbital	N/A		0		
		Rad 1: Ch 1-4 Rad 2: Ch 1-4 Rad 3: Ch 1-4	359004	$< 0.1\%$	
GSFCTV2stable	N/A		0		
		Rad 1: Ch 1-4 Rad 2: Ch 1-4 Rad 3: Ch 1-4	446760	$< 0.1\%$	

Table A.2: *Gain Jitter Test Results (Detection Threshold: 8).*

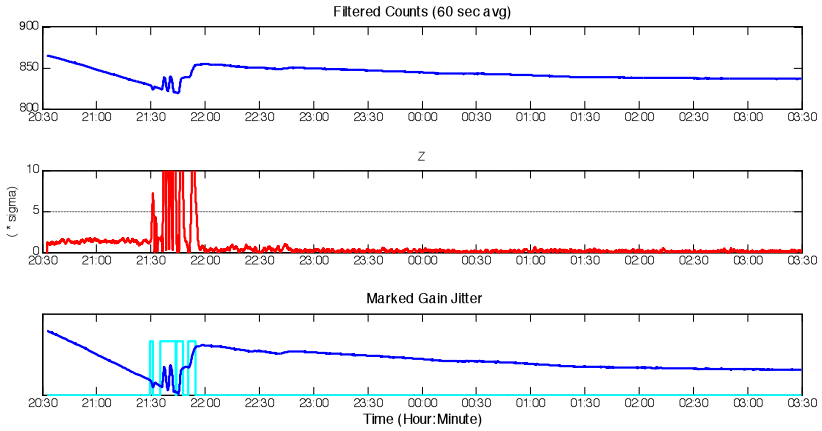

(a)

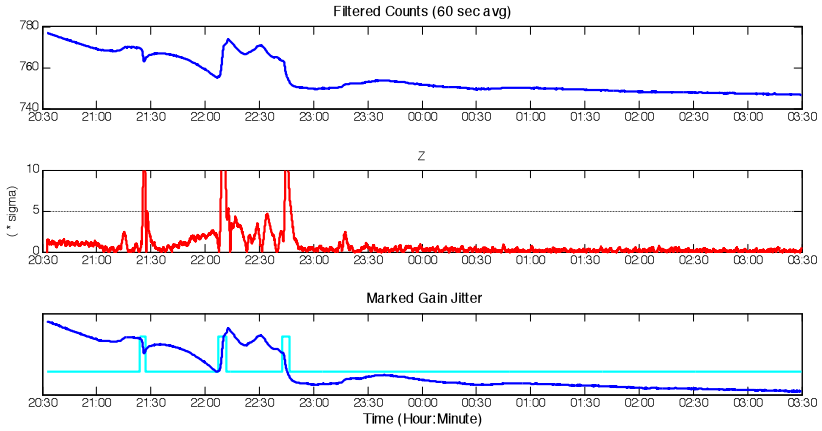

(b)

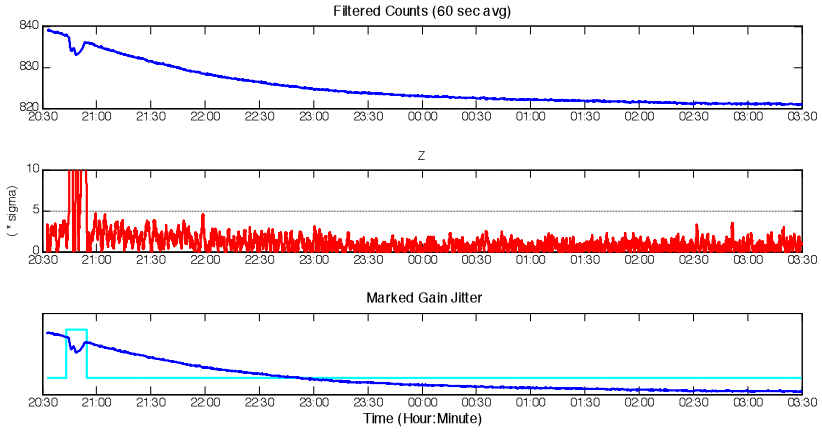

(c)

Figure A.7: *Gain jitter detection with data set JPLradspecial: (a) Radiometer 1, Channel 1; (b) Radiometer 1, Channel 4; (c) Radiometer 2, Channel 4.*

A.5 Conclusion

A gain jitter detection algorithm for the Aquarius radiometers was successfully developed. Three parameters (filter parameters and detection threshold) used in the algorithm were derived by using a training dataset. Additional 3 datasets were used for performance testing. After adjusting the detection threshold (narrowing the range of the detection threshold derived using the training dataset), the gain jitters in the three test datasets could be effectively detected.

A.6 Parameters used in V5.0 product

In the above description, the datasets have 60 second intervals between adjacent samples. For the Aquarius radiometer data to be detected, the actual interval between adjacent samples is 1.44 s, so values of the filter parameters are adjusted correspondingly. N_1 is set to 41 and it results in that the interval between the adjacent samples in the output of the boxcar filter is about 60 s. N_2 is set to 69 which corresponding to 100 s for the parameter Differential Filter Delay in Figure A.4. Note: This setting is equivalent to $N_2 = 2$ for 60 second intervals between adjacent samples. The detection threshold is set to 8.0. The values of the parameter σ in Equation (A.3) for all of the radiometer channels are listed in Table A.3.

	Polarization Channel			
	V	P	M	H
Radiometer 1	0.074	0.048	0.060	0.069
Radiometer 2	0.075	0.048	0.047	0.067
Radiometer 3	0.060	0.047	0.051	0.073

Table A.3: *Standard deviation σ in Equation (A.3).*

References

[1] J. Piepmeier, "Algorithm Theoretical Basis Document for TAA", NASA Technical Document AQU-REF-001505, 2010.

[2] D.M. Le Vine, G.S.E. Lagerloef, F.R. Colomb, S.H. Yueh and F.A. Pellerano, "Aquarius: An Instrument to Monitor Sea Surface Salinity From Space", *IEEE Transactions on Geoscience and Remote Sensing*, vol. 45, no. 7, pp.2040-2050, July 2007.

[3] J. Piepmeier, "Pre-Launch Calibration Test Report", NASA Technical Document AQU-RPT-001317, 2011.

[4] D.M. Le Vine, P. de Matthaeis, C.S. Ruf, and D.D. Chen, "Aquarius RFI Detection and Mitigation Algorithm: Assessment and Examples", *IEEE Transactions on Geoscience and Remote Sensing*, vol.52, no.8, pp.4574-4584, Aug. 2014.

[5] S. Misra and C. Ruf, Detection of Radio Frequency Interference for the Aquarius Radiometer ", *IEEE Transactions on Geoscience and Remote Sensing*, vol. 46, no. 10, pp.3123-3128, October 2008.